B. ONDERKA*, A. DĘBSKI**, W. GĄSIOR**,♯

THERMODYNAMIC ASSESSMENT OF THE Bi-In-Zn SYSTEM

TERMODYNAMICZNY OPIS UKŁADU Bi-In-Zn

A thermodynamic description of the entire ternary Bi-In-Zn system was obtained by the CALPHAD modelling of the Gibbs energy of the liquid phase. The experimental data on the phase equilibria and the thermodynamic properties published and complemented by the authors' own experiments were taken into account. In order to verify the phase equilibria in the Bi-In-Zn system, 15 different samples were studied in the temperature range of 300-900 K by the DTA technique during heating and cooling cycles. Coexisting phases and their composition were analyzed by the SEM and EDX techniques for 9 distinct samples after their thermal equilibration at 373 K and 473 K.

Assessment and selected phase equilibrium calculations were performed with ThermoCalc and Pandat softwares, and compared with experimental data. The obtained results reproduce well the experimental data on both the phase equilibria and the thermodynamic properties in the optimized system.

Keywords: Bi-In-Zn alloys; phase diagram, differential thermal analysis (DTA), phase equilibria

Z pomocą metody Calphad opracowano termodynamiczny model energii swobodnej Gibbsa fazy ciekłej w układzie fazowym Bi-In-Zn, co pozwoliło na termodynamiczny opis tego układu jako całości. Zastosowano własne i literaturowe dane eksperymentalne dotyczące równowag fazowych i właściwości termodynamicznych faz układu trójskładnikowego. W celu weryfikacji uzyskanego opisu wykonano pomiary DTA w zakresie temperatury 300-900 K dla 15 próbek stopów o różnych składach w kolejnych cyklach nagrzewania i studzenia. Równowagę fazową badano analizując technikami SEM i EDX skład fazowy i wzajemną rozpuszczalność składników wygrzewanych izotermicznie stopów w temperaturze 373 K i 473 K.

Optymalizację parametrów modelowych i obliczenia termodynamiczne w układzie Bi-In-Zn wykonano za pomocą oprogramowania ThermoCalc i Pandat. Porównując obliczone równowagi fazowe i funkcje termodynamiczne z danymi doświadczalnymi stwierdzono bardzo dobrą zgodność wielkości eksperymentalnych z właściwościami topologicznymi i termodynamicznymi zoptymalizowanego układu.

1. Introduction

Up till 2007, the thermodynamic data on the ternary Bi-In-Zn system were limited to the early works of Yokokawa et al. [1] and Gluck and Pehlke [2]. Using a galvanic cell with a liquid LiCl+KCl electrolyte, Gluck and Pelke [2] carried out EMF measurements for 16 alloy compositions in the bismuth rich corner in the 723-923 K (450-650°C) temperature range. The sixteen compositions represented the 4 by 4 matrix of the following compositions of zinc and indium in dilute solutions: 1.5, 2.5, 3.37 and 5 at. %. Yokokawa et al. [1] determined the vapour pressures of zinc at 625 K (352°C) for six ternary alloys, with the Zn composition from 0 to 11 at. % using the Knudsen effusion method. The relative error of calculated zinc activity data of these alloys was the estimated of about 4 %. According to the existing experimental data, some of the ternary interaction parameters were optimized by Moelans et al. [3]. However, due to the limited information on the whole

Bi-In-Zn system, they used only the estimated parameters of this ternary system.

Nowadays, two additional papers with the experimental data on the Bi-In-Zn system: the enthalpy of solution [4] and the zinc activity [5] of the liquid Bi-In-Zn solutions have been published. Li et al. [4] determined the integral enthalpies of mixing of liquid Bi-In-Zn alloys at 773 K and 873 K by the drop calorimetric technique in a Calvet-type micro-calorimeter. The concentration of the liquid solutions changed along the nine system sections: Bi:In, In:Zn and Bi:Zn equal 1:1, 1:2 and 2:1, respectively. Unfortunately, the results were shown only graphically in several diagrams. In the present work, the enthalpy data of Li et al. [4] were digitalized directly from those figures, but it seems that such a method of collecting data, even after figure magnification, slightly increases the error of the enthalpy data used for the optimization.

Analyzing the obtained data, Li et al. [4] discovered that the liquid miscibility gap in the ternary system is widened

* AGH UNIVERSITY OF SCIENCE AND TECHNOLOGY, AL. A. MICKIEWICZA 30, 30-059 KRAKÓW, POLAND

** INSTITUTE OF METALLURGY AND MATERIALS SCIENCE, POLISH ACADEMY OF SCIENCES, 25 REYMONTA STR., 30-059 KRAKÓW, POLAND

♯ Corresponding author: w.gasior@imim.pl

by the addition of indium into the Bi-Zn binary liquid alloy. The sample mass loss for all long lasting measurements was within 3% at 773 K and around 5% at 873 K. Additionally, they suggested [4] that the critical temperature, 849 K (576°C), of the Bi-Zn binary system is also the critical temperature of miscibility gap of the ternary Bi-In-Zn system. And so, the ternary miscibility gap will certainly contact the Bi-Zn binary edge in the Gibbs' triangle.

Using the galvanic cell method similar to that used by Gluck and Pehlke's [2], Knott et al. [5] determined the activity of zinc and the excess Gibbs energy of several vertical sections (isopleths) of the ternary Bi-In-Zn system at 873 K. They verified the appearance of the miscibility gap in the ternary system and confirmed that the binary Bi-Zn system miscibility gap extends into the ternary over a certain concentration and temperature range.

However, the information on the phase equilibria of ternary systems is very limited, and this makes the design of an efficient alloy for practical materials very difficult. Therefore, we carried out this work to determine the phase equilibria of the Bi-In-Zn ternary system using the Calculation of Phase Diagrams (CALPHAD) approach with a test of reliability by thermal analysis methods.

2. Experimental procedure and results

In order to verify the phase equilibria in the Bi-In-Zn system, 15 different samples were prepared from 99.999 mass percent In (Indium Corporation, USA) and Bi and Zn, of 99.999 mass percent purity (ITME, Poland). The weighed amounts of pure metals were melted in graphite crucibles in a glove box under purified Ar (impurities <0.1 ppm). After heating up to 773 K (500°C) and mixing of the components, the resulting alloy was cast into a graphite chill. According to such a procedure, the alloys of different molar ratios Bi:In = 1:1, Bi:In = 1:2, Bi:Zn = 1:1 and In:Zn = 1:1 (Table 1) were prepared for differential thermal analyses (DTA). In a similar way, samples of 20 at. % zinc content and a selected Bi:In ratio (Table 2 and 3) were prepared for the equilibration experiments.

2.1. DTA measurements

The system of Bi-In-Zn was studied by the DTA method with the use of a modified MOM Q-1500 (Paulik-Paulik-Erdey) apparatus working up to ~1300 K (~1030°C). The cast alloy samples of about 1 gram were placed in alumina crucibles. The heating and cooling cycle rate of the DTA experiments was 5 K/min in the temperature range of 300 to max. 900 K depending on the temperature of miscibility gap limit (most of alloys were investigated at temperatures lower than 700 K). To avoid the concentration change of alloys due to zinc evaporation, DTA investigations were performed only in one heating and cooling cycle. The partial pressure of Bi and In at 900 K and at lower temperatures is of several order lower in comparison to partial pressure of Zn, therefore their contents shouldn't change considerably during the experiment. The results of the DTA analysis for the samples of the selected compositions are presented in Table 1 (All compositions are in mole fractions or at. percents).

TABLE 1

Results of DTA experiments

Isopleth, molar ratio	Composition along isopleth	Thermal arrests, K	
		heating	*cooling*
Bi:Zn = 1:1	X_{In} = 0.15	384, 685	733, 675, 441, 370
	0.25	385, 678	730, 666, 414, 372
	0.56	345, 354, 363, 654	623, 357, 347
	0.70	325, 347, 358, 601	573, 350
	0.80	356, 388, 534	523, 378
In:Zn = 1:1	X_{Bi} = 0.18	344, 660	708, 648, 353, 339
	0.45	383, 425	665, 416, 368
	0.65	383, 481, 625	595, 468, 372
	0.78	384, 500, 560	548, 369
Bi:In = 1:1	X_{Zn} = 0.15	386	605
	0.45	383, 672	671, 362
	0.75	386, 680	819, 668, 368
Bi:In = 1:3	X_{Zn} = 0.15	346, 363, 620	587, 345, 339
	0.45	351, 655	694, 650, 340, 328
	0.65	348, 654, 667	745, 647, 349, 339

2.2. Isothermal equilibration

The thermodynamic equilibration at 373 K (Tab. 2) and 473 K (Tab. 3) was performed for the samples closed in quartz containers under a slight vacuum. They were prepared by the same procedure as those for the DTA experiments. The equilibration of the alloys was conducted over the period of two months. Next, the samples were fast-cooled in water and prepared for the examination by the electron scanning microscopy.

TABLE 2

Isothermal equilibration at 373 K for samples for X_{Zn} = 0.2

No	Sample concentration		Identified phases
	X_{Bi}	X_{In}	
1	0.65	0.15	(Bi): X_{Bi} = 0.985, X_{In} = 0.015 (Zn)– virtually pure Zn BiIn (no Zn solubility observed)
2	0.22	0.58	(L): X_{Bi} = 0.28, X_{In} = 0.72 (Zn) – virtually pure Zn
3	0.16	0.64	(L): X_{Bi} = 0.212, X_{In} = 0.788 (Zn) – virtually pure Zn
4	0.04	0.76	(In): X_{Bi} = 0.05, X_{In} = 0.95 (Zn) – virtually pure Zn

No	Sample concentration		Identified phases
	X_{Bi}	X_{In}	
5	0.60	0.20	(L): $X_{Bi} = 0.699$, $X_{In} = 0.268$, $X_{Zn} = 0.033$ (Zn) – virtually pure Zn
6	0.45	0.35	(L): $X_{Bi} = 0.485$, $X_{In} = 0.501$, $X_{Zn} = 0.014$ (Bi): $X_{Bi} = 0.983$, $X_{Zn} = 0.017$ (Zn) – virtually pure Zn
7	0.33	0.47	(L): $X_{Bi} = 0.47$, $X_{In} = 0.53$ (Zn) – virtually pure Zn
8	0.58	0.2	(L): $X_{Bi} = 0.273$, $X_{In} = 0.687$, $X_{Zn} = 0.04$ (Zn) – virtually pure Zn
9	0.09	0.71	(L): $X_{Bi} = 0.096$, $X_{In} = 0.839$, $X_{Zn} = 0.065$ (Zn) – virtually pure Zn

The composition of the samples was determined from the EDX analysis (FEI E-SEM XL30) with the internal standards and the ZAF corrections. The observed phases and their compositions are shown in Tables 2 and 3.

The compositions of equilibrated alloys were chosen from previously calculated phase diagram according to binary formalism. The most of samples were chosen in the 2-phase region of equilibrium with ternary liquid solution.

3. Thermodynamic description

3.1. Thermodynamic modelling

During the optimization of the Bi-In-Zn system, the following phases were taken into consideration: liquid solution (L), terminal solid solutions: (Bi), (In), and (Zn) and binary solid phases: BiIn, Bi_3In_5, $BiIn_2$ tetragonal_A6 (α_1-phase). The stable states of Bi, In and Zn at 298.15 K and the pressure of 1 bar (i.e. SER – Standard Element Reference [6]) correspond to the phases: rhombohedral-A7, tetragonal-A6, and hcp-Zn, respectively. The hexagonal structure of Zn (hcp-Zn) should be distinguished from the ideal hexagonal close-packed structure (hcp-A3) because the c/a-ratio (1.86) of Zn deviates considerably from the c/a = 1.63 of the ideal ratio of the hcp-A3 structure.

The substitutional solution model was selected for the tetragonal_A6 phase (α_1), the Liquid phase (L) and the (Bi), (In) and (Zn) rich phases. The Gibbs energy per mole of atoms is expressed as:

$$G_m^{\varphi}(T) = {}^{ref}G_m^{\varphi} + {}^{id}G_m^{\varphi} + {}^{ex}G_m^{\varphi} \tag{1}$$

$$ {}^{ref}G_m^{\varphi} = X_{Bi}\,{}^0G_{Bi}^{\varphi}(T) + X_{In}\,{}^0G_{In}^{\varphi}(T) + X_{Zn}\,{}^0G_{Zn}^{\varphi}(T) \tag{2}$$

$$ {}^{id}G_m^{\varphi} = RT\left(X_{Bi}\ln(X_{Bi}) + X_{In}\ln(X_{In}) + X_{Zn}\ln(X_{Zn})\right) \tag{3}$$

The thermodynamic properties of the ternary solid and liquid solutions were estimated from the assessed description of the binary constituent systems by the Muggianu method [7, 8]:

$$ {}^{ex}G_m^{\varphi} = X_{Bi}X_{In}\sum_i {}^iL_{Bi,In}^{\varphi}(X_{Bi} - X_{In})^i + X_{Bi}X_{Zn}\sum_i {}^iL_{Bi,Zn}^{\varphi}(X_{Bi} - X_{Zn})^i $$
$$ + X_{In}X_{Zn}\sum_i {}^iL_{In,Zn}^{\varphi}(X_{In} - X_{Zn})^i + X_{Bi}X_{In}X_{Zn}\,{}^{ter}L_{Bi,In,Zn}^{\varphi} \tag{4}$$

where ${}^0G_i^{\varphi}$ denotes the Gibbs energy of the pure element i in the structure of the φ-phase:

$$ {}^0G_i^{\varphi} = G_i^{\varphi} - H_i^{SER}(298.15\,K) = $$
$$ = A + BT + CT\ln(T) + DT^2 + ET^{-1} + FT^3 + GT^7 + HT^{-9} \tag{5}$$

$H_i^{SER}(298.15\,K)$ is the molar enthalpy of the stable element reference at 298.15 K and 101,325 Pa, T is the absolute temperature, A–H are the coefficients and X_{Bi}, X_{In} and X_{Zn} are the molar fractions of the Bi, In and Zn φ-phase, respectively. In the present work, the data for the pure elements were taken from the compilation by Dinsdale [9]. The term GT^7 is used only for the liquid below the melting point and the term $+HT^{-9}$ – only for the solid above the melting point [10]. ${}^{ref}G_m^{\varphi}$ is referred to the mechanical mixture of the pure elements in the φ phase at temperature T, ${}^{id}G_m^{\varphi}$ is the Gibbs energy contribution by the ideal entropy of mixing, and ${}^{ex}G_m^{\varphi}$ is the excess Gibbs energy.

The L_{ij} parameters in Eq. (4), often referred to the Redlich-Kister equation [11], are the interaction parameters between the species given in the subscript (i and j) and may be temperature dependent. So, they can be used in a rough form to represent the deviations from the ideal entropy.

The use of the first three terms of Eq. (4) gives the thermodynamic description of ternary phases from respective binaries ("binary formalism") as a first approximation of the ternary phase system. The only possibility to refine the calculated topology of the ternary system according to measured thermodynamic data is to use the ternary interaction parameters which should be optimized according to experimental data obtained for ternary system.

The ternary interaction parameter ${}^{ter}L_{Bi,In,Zn}^{\varphi}$ is composition dependent and has the following form:

$$ {}^{ter}L_{Bi,In,Zn}^{\varphi} = X_{Bi}\,{}^0L_{Bi,In,Zn}^{\varphi} + X_{In}\,{}^1L_{Bi,In,Zn}^{\varphi} + X_{Zn}\,{}^2L_{Bi,In,Zn}^{\varphi} \tag{6}$$

In the COST 531 database [12, 13], the Gibbs free energy of the stoichiometric phases BiIn, Bi_3In_5 and $BiIn_2$ was described on the basis of the assessment of Boa and Ansara [14] by a floating reference state:

$$ {}^0G^{Bi_pIn_q} = p\,{}^0G_{Bi}^{R\,hom\,bohedral-A7}(T) + q\,{}^0G_{In}^{Tetragonal-A6}(T) + A + B\cdot T \tag{7}$$

where: p and q are the stoichiometric coefficients and ${}^0G_{Bi}^{R\,hom\,bohedral-A7}(T)$ and ${}^0G_{In}^{Tetragonal-A6}(T)$ are the standard functions for the elemental Bi and In. This corresponds to the simple assumption of the Kopp-Neumann rule.

3.2. Optimization

In a case of ternary system without ternary phases (i.e. intermetallics) the optimization of system strongly depends on the thermodynamic description of respective binary systems. Thermodynamic data for the binary Bi-In, Bi-Zn and In-Zn systems were taken from the critically assessed thermodynamic model parameters collected in the COST 531 Thermodynamic Database of Lead-Free Solders ver. 3.0 database [13] of the June 2008 version.

The assessment of the Bi-Zn system was based on Malakhov's system optimization [15] with an improvement of the new data for the solubility of Bi in the hcp-Zn terminal phase [16]. The thermodynamic modelling by Lee [17], with

some amendments of the In-Zn interaction parameters of the binary solid phases, was adopted for the In-Zn system.

The Bi-In solid phase described by Moelans [3] β-A6 (in earlier assessments denoted as ε-BiIn [14]) has a tetragonal structure with the c/a-ratio equaling 1.29, which is different from that of pure indium tetragonal structure (A6) with the c/a-ratio of 1.52 at 298.15 K. Thus, an explicit distinction between structure of the phase (In) and the phase β-A6 was accepted. The phase β-A6 is denoted as the α_1-phase (TET_ALPHA1) [12] in the COST 531 database (ver. 3.0). Incongruent melting BiIn$_2$ compound (Tab. 5) was denoted as BiIn_brass in COST 531 database.

No data on the Zn solubility in the α_1-phase has been found in the literature by the time of completion of the present work. Also, no zinc solubility in the binary stoichiometric BiIn, Bi$_3$In$_5$ and BiIn$_2$ phases has been detected. Detailed information on the phases used in the current assessment is summarized in Table 5.

The stable ternary phases of the Bi-In-Zn system have not been reported in the literature up till now. Due to the lack of data on the thermodynamic properties of the terminal solid solutions as well as on their phase boundaries, only the binary contributions were utilized, and the ternary terms were ignored.

The ternary parameters of the liquid phase in the Bi-In-Zn system were assessed taking into account the calorimetric data by Li et al. [4], the Zn activity from the EMF measurements by Knott et al. [5], as well as older data obtained by Gluck and Pehlke [2]. Also, our own data obtained from the thermal analysis were included. All enthalpy data obtained experimentally in [4] were equally used. Especially useful for the CALPHAD optimization of the system were the enthalpies of mixing and the EMF's, as they allow subdividing the excess Gibbs energy of the liquid phase into enthalpic and entropic contributions. A summary of the available experimental data set is given in Table 4.

TABLE 4

Experimental data for ternary Bi-In-Zn system

Experimental method	Ranges of experiment	Reference
EMF (LiCl+KCl electrolyte)	723-923 K 0-5 % at. In, 0-5 % at. Zn	[2]
Knudsen effusion	625 K 0-11 % at. Zn	[1]
Calorimetric	773 K, Bi:In = 1:3, 1:1, 3:1 Bi:Zn = 1:3, 1:1, 3:1 In:Zn = 1:3, 1:1, 3:1	[4]
EMF (LiCl+KCl electrolyte)	873 K and 973 K In:Bi = 1:2, 1:1, 2:1 and 9:1	[5]
DTA	Table 1	This work
Isothermal equilibration	Table 2 and 3	

For this optimization, thermodynamic data for the liquid phase, invariant reactions and liquidus/solidus were used with a certain weight based on personal judgment. The optimization was carried out step by step in agreement with the guideline given by Schmid-Fetzer et al. [18]. On the basis of the experimental data, the ternary parameters of the liquid phase were

evaluated and the Bi-In-Zn system was assessed. First, the optimization of thermodynamic functions of the liquid phase was performed. Then, the invariant reactions were optimized. All parameters were finally evaluated together to provide the best description of the system. For the ternary system optimization, the Parrot module from the ThermoCalc ver. S [6] software was used. Results were checked additionally using Pandat v. 8.1 software [19].

TABLE 5

Details of phases characteristic in the Bi-In-Zn system

Phase	Pearson's Symbol	Constitution
Liquid solution, |L	–	(Bi, In, Zn)
Rhombohedral-A7, (Bi)	hR2	(Bi, In, Zn)
Tetragonal-A6, (In)	tI2	(Bi, In, Zn)
hcp-Zn, (Zn)	hP2	(Bi, In, Zn)
BiIn	tP4	$(Bi)_{1/2}(In)_{1/2}$
Bi$_3$In$_5$	tI32	$(Bi)_{3/8}(In)_{5/8}$
BiIn$_2$	hP6	$(Bi)_{1/3}(In)_{2/3}$
Tetragonal-A6, (α_1), *former ε-BiIn or β-A6* [3]	tI2	(Bi, In)

3.3. Optimization Results

The results of the present evaluation are collected in Table 6 and shown in Figs. 1-9, together with a comparison of the calculated data with our own experimental data and the recent literature data of [4] and [5]. It should be noted that, in the cited paper [4], the experimental enthalpy data have been only presented as the composition dependent diagrams.

TABLE 6

Summary of thermodynamic ternary parameters of liquid phase of Bi-In-Zn system according to the present optimization

Phase	Function
$^0L^L_{Bi,In,Zn}$	-11397.1+0.798· T
$^1L^L_{Bi,In,Zn}$	7495.8
$^2L^L_{Bi,In,Zn}$	-19544.9+16.220· T

Since the CALPHAD approach allows for the calculation of thermodynamic functions, a comparison of the calculated enthalpy of mixing at different atomic ratios with the experimental data of the liquid Bi-In-Zn alloys of Li et al. [4] is shown at the temperature of 773 in Figs. 1-3 for three different elements ratio: 1:2, 1:1 and 2:1. Besides the narrow Zn-poor composition range (X_{Zn} <0.15 at Bi:In vertical section) this enthalpy data show a positive deviation from the ideal solution for the samples with a relatively high concentration of the volatile elements as Bi and Zn, with the melting temperatures of 544.5 K (271.4°C) and 692.6 K (419.5°C), respectively. An abnormal dependence of the enthalpy of mixing on the concentration was observed for the Bi:In vertical sections (Fig. 1) and for Bi:Zn and In:Zn ratios: 1:2 (Fig. 3) [4]. It was deduced [4] that the abrupt kinks represent the limits of miscibility gap of Bi-In-Zn system at 773 K. The

experimental limits of the miscibility gap are very well repro-duced with the use of the present thermodynamic description in Figs. 1-3. The difference between the calculated and the experimental enthalpy values in the miscibility gap area is probably due to the unfinished phase separation of the liquid solution. Such separation seems to decrease with the increas-ing In concentration in liquid melt what can be observed for the bismuth concentration $X_{Bi} > 0.3$ at the In:Zn =1:2 vertical section (Fig. 3).
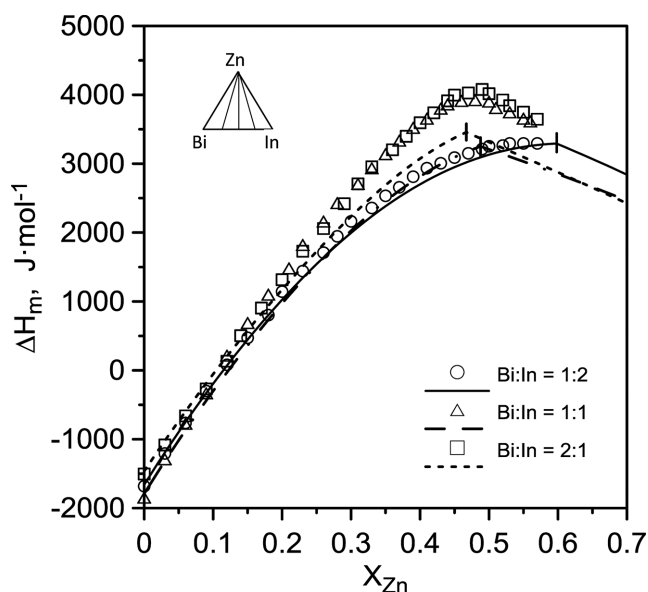

Fig. 1. Comparison of calculated enthalpy of mixing and experimen-tal data of Li et al. [4] of liquid Bi-In-Zn alloys at 773 K and for atomic ratio Bi:In = 1:1, Bi:In = 1:2 and Bi:In = 2:1. The limits of the miscibility gap was denoted by vertical short lines
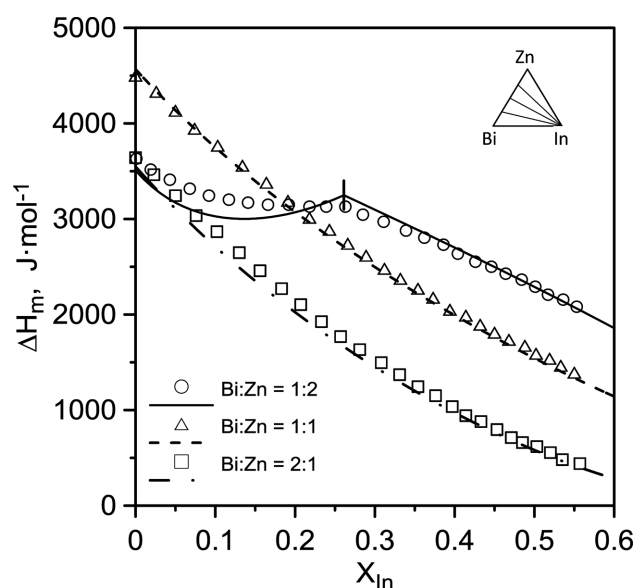
Fig. 2. Comparison of calculated enthalpy of mixing and experimen-tal data of Li et al. [4] of liquid Bi-In-Zn alloys at 773 K and for the atomic ratio: Bi:Zn = 1:2, Bi:Zn = 1:1 and Bi:Zn = 2:1. The limits of the miscibility gap was denoted by vertical short lines
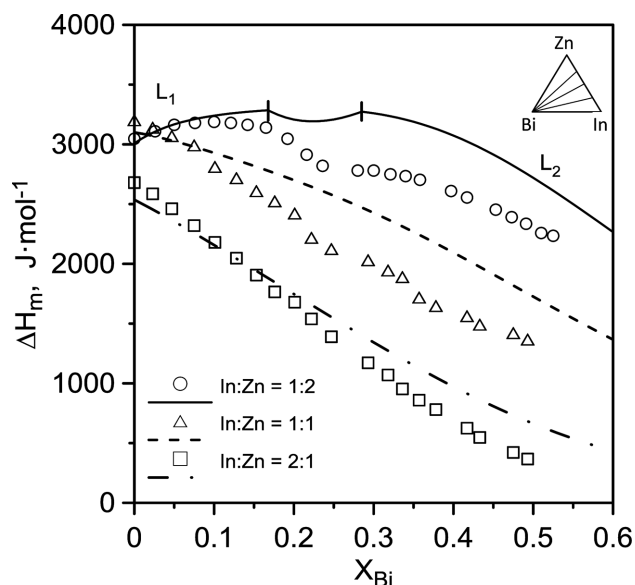
Fig. 3. Comparison of calculated enthalpy of mixing with experimen-tal data of Li et al. [4] at 773 K for mole ratio: In:Zn = 1:2, In:Zn = 1:1 and In:Zn = 2:1. The limits of the miscibility gap was denoted by vertical short lines

Most of the experimental and the calculated enthalpies of mixing obtained for Bi:In and Bi:Zn vertical sections fit very well, in contrast to the enthalpy data of the liquid Bi-In-Zn measured for the In:Zn isopleth [4] (Fig. 3). The biggest differ-ence between experimental and the calculated data for In:Zn = 1:1 and for L_2 concentration range of In:Zn =1:2 isopleth does not exceed ~500 J/mol. It seems that Bi addition to Zn-rich liquid L_1 results in an effect of poor mixing of the heavy metal in solution, probably because of gravitational separa-tion in stirrer free calorimeter [4]. Such discrepancy was also observed at the temperature 873 K, but the highest difference for this ratio observed in the concentration range of 30-55 at. % Bi is not more than ~1 kJ/mole. Anyway, all differences do not exceed the range of a typical calorimetric experimental uncertainty, ±500 J/mole. Additionally, the calculated results very well reproduce the shape of experimental concentration dependence in range of the experimental error.

A comparison of the e.m.f. values calculated and deter-mined experimentally by Knott et al. [5] is shown in Figs. 4 and 5. During the optimization of the liquid phase, the higher weight was used for the low zinc concentration e.m.f. data. For high zinc concentrations (Fig. 4(b)), the experimental error, ±1 mV, is almost equal to the measured e.m.f of the galvanic concentration cell. Additionally, for these data, the calculated e.m.f vs. T dependences show kinks at the liquidus in a low temperature range (Figs. 4(b)). It should be noted that, in the cited paper [5], the e.m.f data have only been presented as the linear functions obtained from the experimental data by the least squares method with the 5% fitting error.

The comparison of the calculated electromotive force of the concentration cells for all molar rates of the elements of the Bi-In-Zn system with the experimental data of Knott et al. [5] (Figs. 4 and 5) shows a very good agreement in the experimental error range for the Zn concentration up to 50%. Above this zinc concentration value, the difference between the calculated and the experimental data can be observed. How-ever, with the consideration of the experimental and fitting

errors, it was found that the optimized parameters describe the thermodynamic properties of the liquid phase very well.
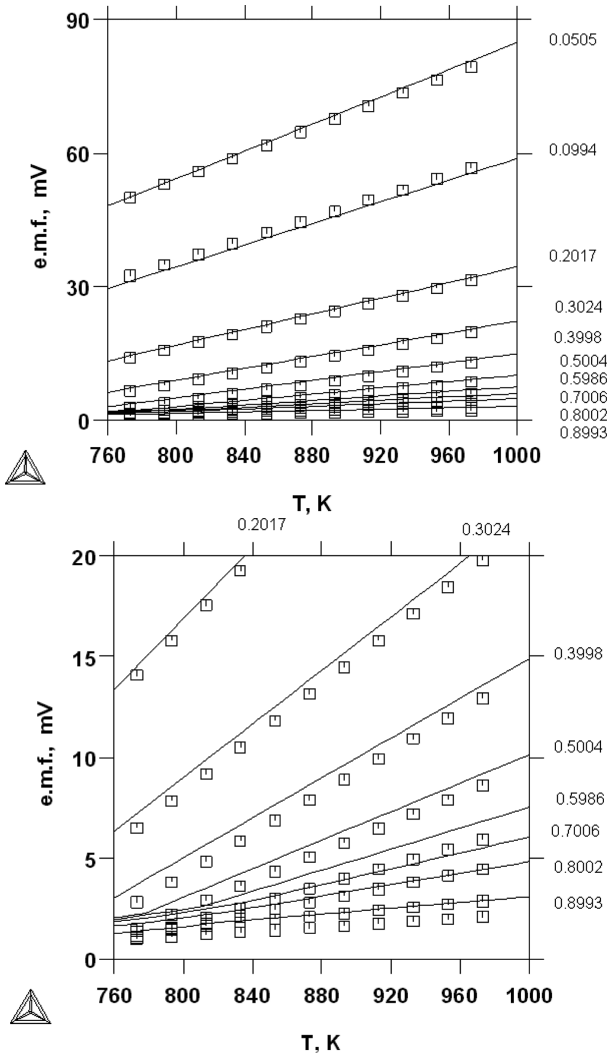

Fig. 4. a) Comparison of e.m.f. vs. T dependence calculated from assessed parameters for molar rate Bi:In = 1:1 and different Zn contents (assigned at the right side) with experimental results of [5]; b) High zinc composition part of diagram. The kink at the e.m.f. vs. temperature dependence denotes a liquidus temperature
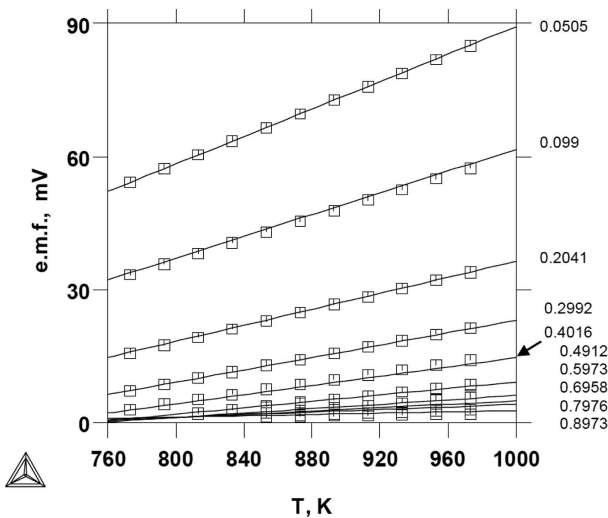

Fig. 5. Comparison of e.m.f. vs. T dependence calculated from assessed parameters for molar rate Bi:In = 1:2 and different Zn contents (assigned at the right side) with experimental results of [5]

It should be noted that the experimental e.m.f data of Gluck and Pehlke [2] at 823 K for selected indium contents: X_{In} = 0.015, 0.025, 0.0375, 0.05 and different Zn concentrations in dilute solutions showed a maximum difference with the calculated values of only 5% for X_{Zn} = 0.05.

The zinc activity data obtained from results of Yokokawa et al. [1] at 625 K (352°C) for six ternary alloys for the Zn composition from 0 to 11 at. % were compared with calculated values in Fig. 6. Taking into account substantial uncertainty of Knudsen effusion method it seems that overall agreement is satisfactory.
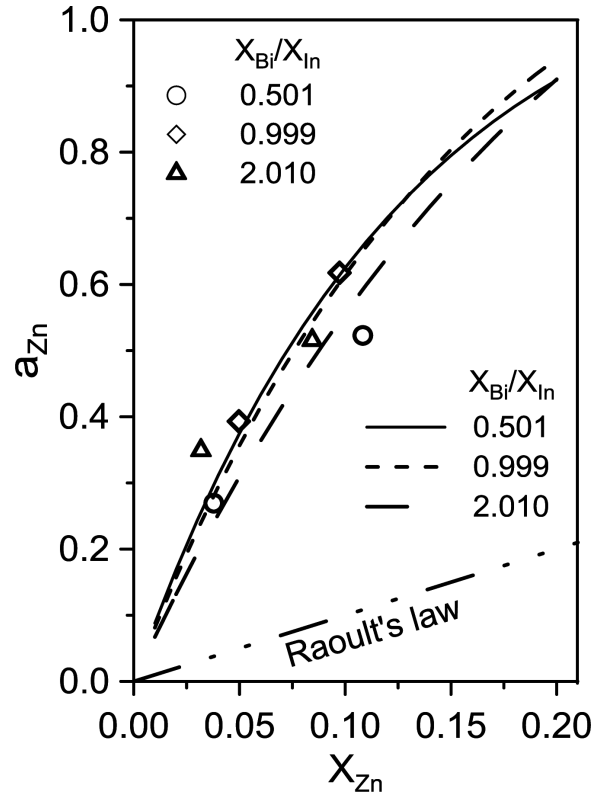

Fig. 6. The zinc activity data obtained from results of Yokokawa et al. [1] at 625 K for six ternary alloys for the Zn composition from 0 to 11 at. % compared with calculated

Figure 7(a) shows the extensive liquid miscibility gap with a flat maximum near the critical point close to the Bi-Zn binary system. The critical point coordinates were estimated to be: 5.89 at. % Bi, 4.98 at. % In, 89.13 at. % Zn and 875.5 K (602.4°C). So the critical point is very near Bi-Zn binary edge in the Gibbs triangle and 26.5 K higher than the critical point miscibility gap of the Bi-Zn binary system (849 K). The comparison of the calculated liquidus projection diagram with the experimental data of the miscibility limit estimated from the enthalpy of solution data at 773 K [4] shows very good coherence. The liquidus isothermal sections are shown every 20 K and the invariant reactions are denoted according to Table 7. Letter m denotes the lowest temperature of monotectic reaction $L_1 \leftrightarrow L_2 +$ (Zn) and the lines represent the liquidus valleys. The magnified zinc-lean part of the Bi-In-Zn diagram with invariant reactions together with the 5 K liquidus surface isothermal sections has been presented in Fig. 7 (b). The solid line in the right part of the diagram indicates the maximum of indium content in Bi-In-Zn system.
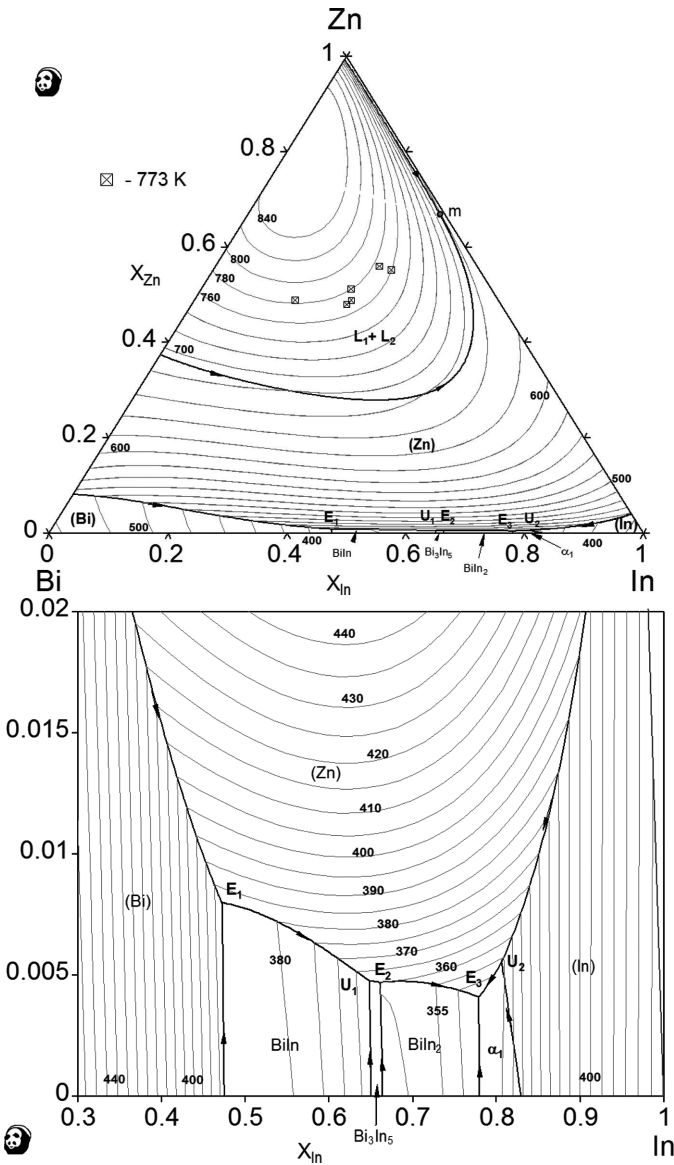
Fig. 7. (a) Liquidus projection of Bi-In-Zn system calculated according to assessed model parameters. Liquidus isotherms calculated every 20 K. Invariant reactions denoted according to Table 7. The experimental data of miscibility gap boundary at 773 K [4] (⊠) were superimposed. Letter m denotes the lowest temperature of monotectic reaction $L_1 \leftrightarrow L_2 + (Zn)$. Lines represent the liquidus valleys; (b) Magnified Zn-lean part of Bi-In-Zn system with 5 K liquidus surface isothermal sections. The solid line in the right part of the diagram indicates the end of the system. Invariant reactions denoted according to Table 7. Lines represent the liquidus valleys
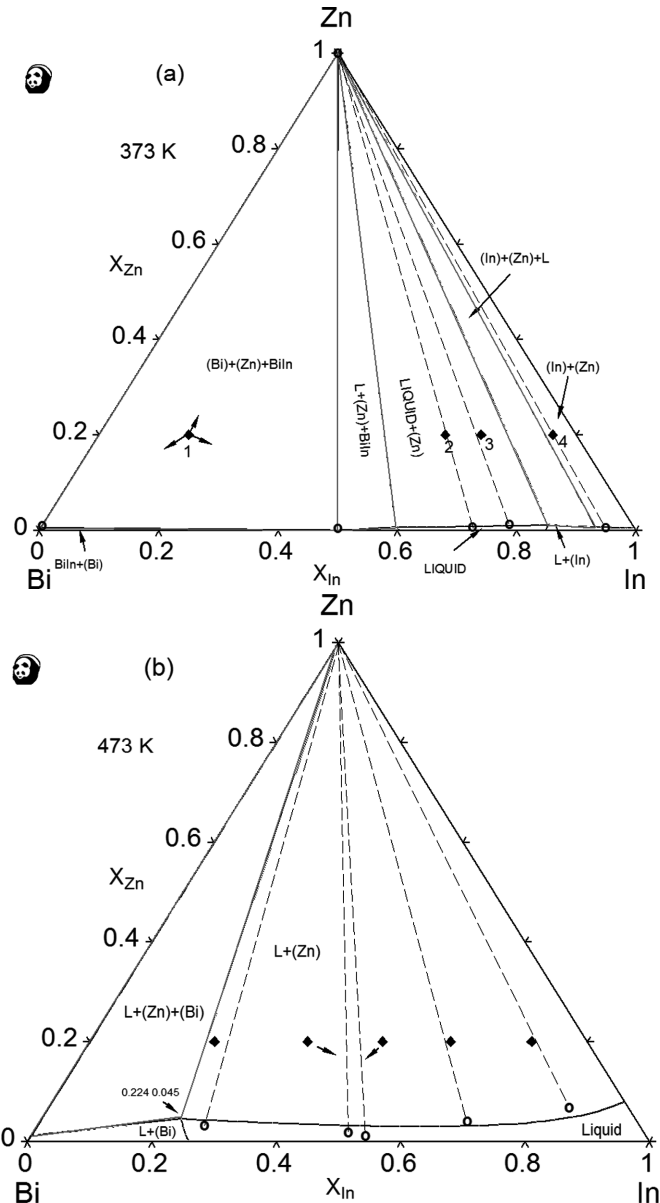

Fig. 8. Isothermal sections of ternary Bi-In-Zn system calculated at: (a) 373 K and (b) 473 K. The experimental data for the solubility of the components in some phases at relevant temperatures after isothermal equilibration (○) (Table 2 and 3) were superimposed together with the nominal alloy compositions (◆)

The results obtained from the isothermal equilibration for the ternary Bi-In-Zn system at 373 K and 473 K (Tab. 3 and 4) are shown together with the nominal sample alloy concentrations at the calculated isothermal sections in Figs. 8(a) and 8(b). The concentrations of equilibrated phases determine the ends of tie lines in two phase region and fit very well with the nominal alloy sample concentrations at 373 K and with the calculated concentration of liquid solution. Only two samples at 473 K of $X_{Zn} = 0.2$ nominal concentration and $X_{Bi} = 0.45$, and 0.58 show slight difference denoted by arrows.

In order to test the calculated univariant and invariant temperatures, DTA measurements for selected alloy compositions were performed. The results were superimposed on the Bi-In-Zn vertical sections in Figs. 9(a)-(d) and were used as an additional verification of the calculated phase diagrams. The calculated univariant and invariant lines agree very well with the phase boundaries confirmed by the DTA measurements.

In the Bi-In-Zn system, three ternary eutectic reactions, $E_1 \div E_3$ (class I reaction [19, 20]), and two U-type (class II) reactions, U_1 and U_2, with a part of the liquid solution were calculated. The temperature of U_3: $(Zn)+\alpha_1 \leftrightarrow (In)+BiIn_2$ invariant reaction calculated from the assessed parameters at 324.7 K (51.55°C) can be connected with the DTA thermal arrest at the temperature of 325 K (Tab. 1, Fig. 9b).

TABLE 7

Invariant reactions in Bi-In-Zn system. Comparison with invariant temperatures estimated by Moelans et al. [3]

| Type	Reaction	T, K		Present data			
				Equilibrium composition of liquid solution		Equilibrium composition of phase α_1	
		This work	[3]	X_{Bi}	X_{In}	X_{Bi}	X_{In}
E_1	L $\leftrightarrow$ (Bi)+BiIn+(Zn)	380.9	381.0	0.520	0.472	–	–
U_1	L+BiIn $\leftrightarrow$ (Zn)+Bi$_3$In$_5$	360.8	360.0	0.347	0.648	–	–
E_2	L $\leftrightarrow$ (Zn)+Bi$_3$In$_5$+BiIn$_2$	359.9	358.9	0.334	0.661	–	–
U_2	L+(In) $\leftrightarrow$ (Zn)+α_1	353.7	341.0	0.189	0.806	0.119	0.881
E_3	L $\leftrightarrow$ (Zn)+BiIn$_2$ + α_1	343.7	–	0.218	0.778	0.151	0.849
E_3	L $\leftrightarrow$ (In)+BiIn$_2$+(Zn)	–	340.8	0.218	0.778	–	–
U_3	(Zn)+α_1 $\leftrightarrow$ (In)+BiIn$_2$ Fig. 9(c, d)	324.7	–	–	–	0.117	0.883
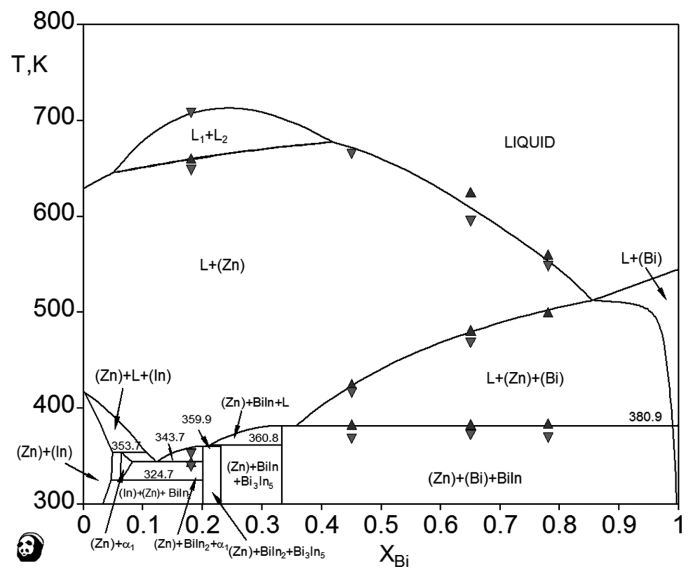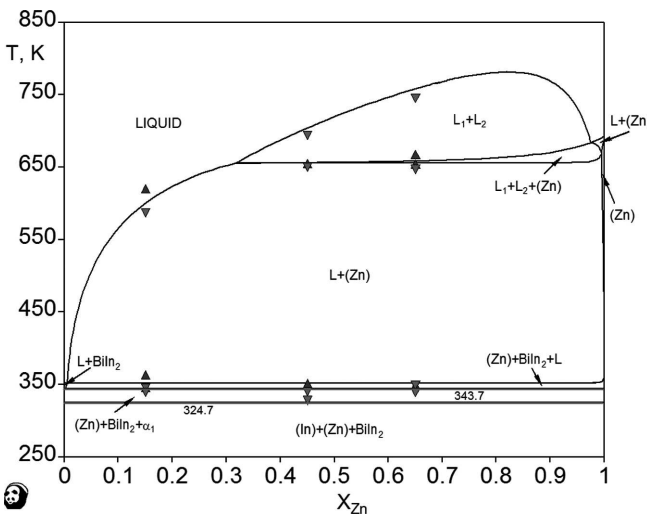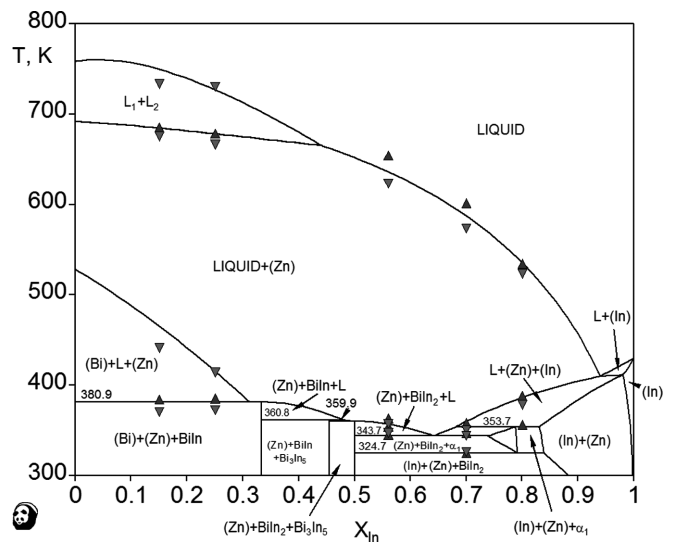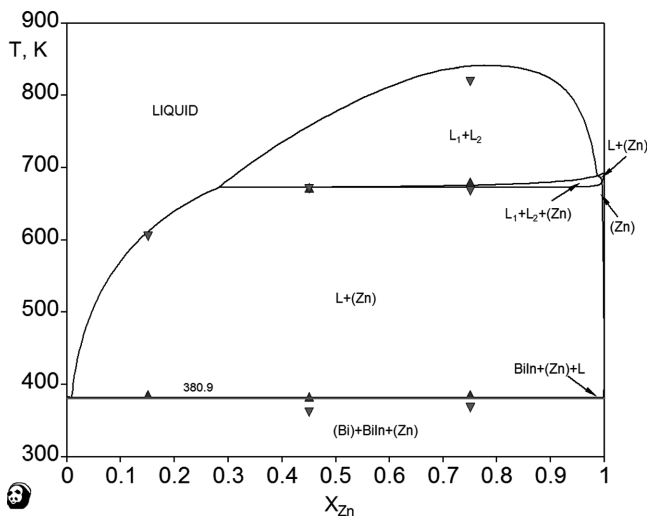
Fig. 9. Vertical section of Bi-In-Zn system for: a) Bi:In = 1:1; b) Bi:In = 1:3; c) Bi:Zn = 1:1; d) In:Zn = 1:1. The experimental DTA signals registered during cooling, ▼, and heating, ▲, cycles were superimposed

The calculated temperatures of the invariant reactions in the Bi-In-Zn system are also compared with the values estimated by Moelans et al. [3] in Table 7. The maximum difference of the invariant temperatures is ~3.6% for reaction U_2: L+(In) $\leftrightarrow$ (Zn)+α_1.

In the present assessment, the products of the eutectic reaction E_3 (343.7 K) are the phases (Zn), BiIn$_2$ and α_1, in contrast to the (In) phase calculated from Moelans et al. [3] (340.8 K). However, the concentration of the liquid phase present in the E_3 reaction is identical for the compared optimizations (Tab. 7). The additional solid state reaction U_3: (Zn)+α_1 $\leftrightarrow$ (In)+BiIn$_2$ at 324.7 K was calculated for the assessed system. The reactions E_3 of [3] and U_3 are very close in the liquidus projection diagram (Fig. 7(b)), and a relatively slight change in the Gibbs energy of the liquid phase can produce a topology change in that part of the system. The precipitation of solid phases in solid state reactions at low temperatures are rather slow but it seems that the existence of the U_3 reaction was confirmed by the DTA analysis at 325 K (Tab. 1, Fig. 9(b)) for Bi:In vertical section. From this figure one can find that the calculated phase diagram is in very good agreement with the experimental data.

A further improvement could be achieved by the introduction of ternary parameters for the terminal solid solutions, yet, owing to the lack of experimental data, this would be, at present, inappropriate.

4. Conclusions

A thermodynamic evaluation of the entire ternary system Bi-In-Zn was carried out, involving the following information:
- a study of the phase transition temperatures in the temperature range of 300-900 K by the analysis of 15 distinct samples by the DTA method during 5 K/min heating and cooling cycles.
- a determination of the phase constituents and composition of the coexisting phases of 9 samples by the SEM and EDX techniques after their thermal equilibration at 373 K and 473 K.
- a thermodynamic description of the ternary Bi-In-Zn system by the CALPHAD modelling, with the consideration of the relevant experimental data on ternary Bi-In-Zn alloys existing in the literature and obtained from the above mentioned measurements.
- thermodynamic equilibrium calculations of the liquidus surface, the isothermal sections, the isopleths and selected thermodynamic properties, compared with the experimental data.

The reliability of the assessed parameters obtained for the Bi-In-Zn system was verified by the calculation of the thermodynamic properties as well as the vertical and isothermal sections of the phase diagram. These results were compared with the experimental data, both from our work and the literature [1, 2, 4 and 5]. Our own experimental results led to the verification of the invariant reactions and the univariant lines (liquidus, solidus and solvus) of the Bi-In-Zn phase diagram.

The agreement between the calculated and experimental phase and the thermodynamic data is very good for a broad set of experimental measurements carried out by different authors. Deviations of the experimental and the calculated points are mainly within the limit of the experimental errors.

The derived thermodynamic description of the system can be very useful in the future optimization of the quaternary Bi-In-Sn-Zn system.

REFERENCES

[1] T. Yokokawa, A. Doi, K. Niwa, J. Phys. Chem. **65**, 202-205 (1961).
[2] J.V. Gluck, R.D. Pehlke, Trans. AIME **239**, 36-47 (1967).
[3] N. Moelans, K.C.H. Kumar, P. Wollants, J. Alloys Compd. **360**, 98-106 (2003).
[4] Z. Li, S. Knott, A. Mikula, Acta Mater. **55**, 2417-2422 (2007).
[5] S. Knott, Z. Li, C.-H. Wang, A. Mikula, Met. Mater. Trans. A **41A**, 3130-3135 (2010).
[6] H.L. Lukas, S.G. Fries, B. Sundman, Computational Thermodynamics, The Calphad Method, Cambridge University Press, ISBN 978-0-521-86811-2, 2007.
[7] B. Sundman, B. Jansson, J.O. Andersson, Calphad **9**, 153-190 (1985).
[8] Y.M. Muggianu, M. Gambino, J.-P. Bros, J. Chim. Phys. **72**, 83-88 (1975).
[9] A.T. Dinsdale, Calphad **15**, 317-425 (1991).
[10] J.O. Andersson, A.F. Guillermet, P. Gustafsson, M. Hillert, B. Jansson, B. Jonsson, B. Sundman, J. Ågren, Calphad **11**, 93-98 (1987).
[11] O. Redlich, A.T. Kister, Ind. Eng. Chem. Res. **40**, 345-348 (1948).
[12] A. Kroupa, A.T. Dinsdale, A. Watson, J. Vrestal, J. Vízdal, A. Zemanova, JOM **59**, 20-25 (2007).
[13] A. Dinsdale, A. Watson, A. Kroupa, J. Vrestal, J. Zemanova, J. Vizdal, COST 531 – Lead Free Solders. Vol. 1, Atlas of Phase Diagrams for Lead-Free Soldering, European Report COST 531, Brno 2008, ISBN 978-80-86292-28-1.
[14] D. Boa, I. Ansara, Thermochim. Acta **314**, 79-86 (1998).
[15] D.V. Malakhov, Calphad **24**, 1-14 (2000).
[16] J. Vizdal, M.H. Braga, A. Kroupa, K.W. Richter, D. Soares, L.F. Malheiros, J. Ferreira, Computer Coupling of Phase Diagrams and Thermochemistry **31**, 438-448 (2007).
[17] B.J. Lee, Calphad **20**, 471-480 (1996).
[18] R. Schmid-Fetzer, D. Andersson, P.Y. Chevalier, L. Eleno, O. Fabrichnaya, U.R. Kattner, B. Sundman, C. Wang, A. Watson, L. Zabdyr, M. Zinkevich, Calphad **31**, 38-52 (2007).
[19] W. Cao, S.-L. Chen, F. Zhang, K. Wu, Y. Yang, Y.A. Chang, R. Schmid-Fetzer, W.A. Oates, Calphad **33**(2), 328-342 (2009).
[20] F.N. Rhines, Phase Diagrams in Metallurgy, McGraw-Hill Book Comp., NY, 1956.
[21] A. Prince, Alloy Phase Equilibria, Elsevier, Amsterdam, p. 211, 1966.